Available online at www.sciencedirect.com
SCIENCE DIRECT®
Biochimica et Biophysica Acta 1605 (2003) 83–95
BIOCHIMICA ET BIOPHYSICA ACTA
BBA
www.bba-direct.com

Stark spectroscopy of the light-harvesting complex II in different oligomerisation states

Miguel A. Palacios[a,*], Raoul N. Frese[a], Claudiu C. Gradinaru[a,b], I.H.M. van Stokkum[a], Lavanya L. Premvardhan[a], Peter Horton[c], Alexander V. Ruban[c,d], Rienk van Grondelle[a], Herbert van Amerongen[a,e]

[a] *Department of Biophysics and Physics of Complex Systems, Division of Physics and Astronomy, Faculty of Sciences, Vrije Universiteit, De Boelelaan 1081, 1081 HV Amsterdam, The Netherlands*
[b] *Department of Biophysics, Leiden University, Niels Bohrweg 2, 2333 CA Leiden, The Netherlands*
[c] *Department of Molecular Biology and Biotechnology, Robert Hill Institute, University of Sheffield, Western Bank, Sheffield S10 2TN, UK*
[d] *UMR 8543, Departement de Biologie, Ecole Normale Superieure, 45 Rue D'Ulm, 75230, Paris, Cedex 05, France*
[e] *Laboratory of Biophysics, Department of Agrotechnology and Food Sciences, Wageningen Universiteit, Dreijenlaan 3, 6703 HA Wageningen, The Netherlands*

Received 28 January 2003; received in revised form 13 June 2003; accepted 19 June 2003

Abstract

The electric field-induced absorption changes (Stark effect) of light-harvesting complex II (LHCII) in different oligomerisation states—monomeric, trimeric and aggregated—have been probed at 77 K. All the chlorophyll (Chl) *a* molecules exhibit electro-optic properties in the Q_y absorption region characterized by a change in dipole moment $|\Delta\vec{\mu}| = 0.6 \pm 0.06\ D/f$ and polarizability, $\mathrm{Tr}(\Delta\tilde{\alpha}) \sim 55 \pm 5\ \text{Å}^3/f^2$ upon electronic excitation, which are similar to those of unbound monomeric Chl *a*, indicating the absence of strong delocalization of the excitations which would be expected in the presence of strong excitonic interactions. The Stark effect in the Chl *b* absorption region is significantly bigger with $|\Delta\vec{\mu}|$ values of the order of 2.0 ± 0.2 D/*f* and it is attributed to strong interactions with neoxanthin molecules. Clear oligomerisation-dependent differences are observed in the carotenoid region, mainly due to the appearance of a new xanthophyll absorption band at 509 in the spectra of trimers and oligomers. It is ascribed to some lutein molecules, in agreement with previous experimental observations. The electro-optic properties of these lutein molecules are significantly different from those of the other xanthophylls in LHCII, which do not exhibit such a big change in dipole moment upon electronic excitation ($|\Delta\vec{\mu}| = 14.6 \pm 2.0$ D/*f*). Upon aggregation of LHCII some extra absorption appears on the red side of the main Chl *a* Q_y absorption band. In contrast to an earlier suggestion [J. Phys. Chem., A 103 (1999) 2422], no indications are found for the charge-transfer character of the corresponding band. The assignments of the S_2 electronic transitions of neoxanthin and lutein in LHCII and possible origins of the Stark effect are discussed.

Keywords: LHCII; Stark; Carotenoid; Xanthophyll; Lutein; Neoxanthin; Charge-transfer state

1. Introduction

Photosynthesis is the process in which sunlight energy is absorbed by plants and bacteria and used to synthesize organic compounds. In order to perform the reactions involved in this process plants are equipped with two photosystems (PSI and PSII). Most of the pigments in PSII are bound to the major peripheral light-harvesting complex II (LHCII) [1,2]. This complex is binding more than 40% of chlorophyll in the photosynthetic membrane and is involved in light harvesting and photoprotection. LHCII is largely organized in trimers and on average four trimeric units are present per PSII reaction center [3]. Seven to eight Chl *a* molecules, five to six Chl *b*, two luteins, one neoxanthin and trace amounts of violaxanthin per monomeric unit are usually bound to this complex [3]. Violaxanthin bound at

Abbreviations: Chl, Chlorophyll; IEF, isoelectric focusing; LHCII, light-harvesting complex II; CD, circular dichroism; LD, linear dichroism; T−S, triplet minus singlet; w/v, weight per volume; v/v, volume per volume; PSI, photosystem I; PSII, photosystem II

* Corresponding author. Tel.: +31-20-444-7935; fax: +31-20-444-7899.
E-mail address: miguelan@nat.vu.nl (M.A. Palacios).

0005-2728/03/$ - see front matter © 2003 Elsevier B.V. All rights reserved.
doi:10.1016/S0005-2728(03)00080-X

the periphery of the complex is easily removed upon isolation [4–7]. Monomeric units or aggregates of this complex can also be obtained by several biochemical procedures and changes in aggregation lead to small but significant changes in the optical properties [8–13]. Most likely, variation in the degree of oligomerisation also occurs in vivo and is related to photoprotective regulation mechanisms like nonphotochemical quenching (NPQ) [4,14].

The structure of LHCII was resolved at a resolution of 3.4 Å by Kühlbrandt et al. [15] and an atomic model was proposed, which constituted an important step for understanding the functional properties of LHCII and for correlating the structure to the spectroscopic properties. The closest distances between the Chl molecules fall in the range 8.3–10.5 Å and two luteins are present in the center of the complex, which have an important role in stabilizing the complex [16]. A third xanthophyll, namely neoxanthin, was not observed in the crystal structure but Croce et al. [17] have determined its approximate orientation and position to be next to two Chl *b* molecules, close to helix C. In spite of the close distances between some Chl molecules, no strong excitonic interactions seem to be present although chlorophylls and xanthophylls influence their mutual spectroscopic properties to some extent [12,17–20].

The optical and functional properties of LHCII are influenced by both pigment–pigment and pigment–protein interactions. The complex has been studied by means of many steady-state and time-resolved spectroscopic techniques (for a review see Ref. [18]), which has led to a general understanding of the origin of the absorption band composition and the flow of excitation energy. However, many details of the pigment ensemble properties and work are still missing, partly because no high-resolution crystal structure is available. It appears that differences in pigment site energies are partly responsible for the absorption fine structure that can be observed at cryogenic temperatures, but also excitonic interactions between pigments are contributing [10,18,20–22]. On the other hand, homogeneous and inhomogeneous broadenings (100–200 cm^{-1}) are of comparable magnitude as the largest excitonic interactions, which explains why the amount of delocalization upon excitation appears to be small [18,19,21,23–25].

The Chl *a* molecules are responsible for the absorption between 660 and 680 nm, whereas the Chl *b* pigments show major absorption in the region between 640 and 660 nm. By means of low-temperature (polarized) absorption spectroscopy it is possible to resolve distinct bands: 661, 668, 671, 673, 676, 680 nm (Chl *a*) and 640, 647, 649, 652 and 656 nm (Chl *b*) [10,11,13,25,26]. Monomers of LHCII usually exhibit more red absorption than trimers, with a maximum at ~677 nm [10,27]. Additionally, there is an increase in absorption around 662 nm and a lack of fine structure in the circular dichroism (CD) and linear dichroism (LD) spectra in the Chl *b* region (loss of bands at 647 and 652 nm). Aggregation leads to the appearance of new red bands [10,11,28], but at the same time to the flattening of the absorption spectrum due to light scattering and a non-random distribution of trimers in the volume probed by the monitoring beam (the sieve effect) [29,30]. Fluorescence spectrum of LHCII aggregates is characterized by a shoulder or maximum at 700 nm in addition to the main peak at 680 nm at 77 K for trimers, and by a reduction in the fluorescence quantum yield (see for instance Ref. [8]). The mechanism of the fluorescence quenching in aggregates remains unclear. Different models have been proposed: changes in the Chl *a*-carotenoid interactions [18,31], the formation of Chl *a* dimers or excimers which are weakly fluorescent or nonfluorescent [32,33] and the presence of a charge-transfer state acting as a trap for the excitations [28].

Electronic transitions associated with the different types of LHCII anthophylls have been determined by low temperature (polarized) absorption, T – S absorption measurements and by Resonance Raman spectroscopy on the wild type and reconstituted LHCII samples. Regarding the S_2 $0 \rightarrow 0$ transition, lutein absorbs at 494 and 510 nm in trimers, but upon monomerization the 510-nm band is lost [5,7,12,34]. Neoxanthin is responsible for the absorbance at ~486 nm and violaxanthin, which can bind at two different sites in LHCII, absorbs mainly at ~488 nm [5,7,12].

In this work we present Stark measurements on LHCII in different oligomerisation states to gain more insight in the relative contributions of pigment–pigment and pigment–protein interactions and the differences in spectroscopic properties of LHCII in different oligomeric states. Previous Stark measurements were restricted to one kind of oligomerisation state and the lack of a structural model hampered the correlation between structure and experimental results [35]. Here we characterize the properties of the xanthophyll electronic states and also probe the presence of the charge-transfer states in oligomeric LHCII as possible cause of the fluorescence quenching.

2. Materials and methods

2.1. Sample preparation

LHCIIb was prepared from spinach BBY (PSII-enriched) particles using isoelectric focusing (IEF) [36]. Purification of trimers and removal of violaxanthin was carried out using sucrose gradient technique [4]. Monomeric LHCIIb was obtained by 48-h incubation of trimers with phospholipase and separation from trimers by sucrose gradient centrifugation. Small aggregates of LHCIIb with minimized light scattering were obtained by removal of detergent using biobeds resin (BioRad). The sample of LHCII in trimeric state was placed in a stirred cell for the room temperature fluorescence measurements. The intense fluorescence signal was constantly monitored. Sixty milligrams of biobeds was added to a cell and mixed with the sample. After approximately 15 min steady and relatively slow ($t_{1/2}$ = 15 min) decrease in the fluorescence signal took place. After achiev-

ing 75% of the fluorescence quenching the sample was quickly removed from the cell. The remaining biobeds were separated form the sample by spinning down in the microfuge for 1 min. The average size of LHCII aggregates obtained by this procedure was found to be 27.0 ± 6.0 nm using the negative staining electron microscopic analysis. Large LHCII aggregates were obtained by prolonging incubation of the sample in biobeds to achieve the fluorescence quenching of 85–90% or by using the overnight dialysis against the detergent-free buffer. These procedures created the 2D lamellar aggregates as described earlier by Ruban and Horton [8].

The pigment stochiometries in every sample were approximately 8 Chl *a*, 6 Chl *b*, 2 luteins and 1 neoxanthin per monomeric subunit. There was no zeaxanthin or violaxanthin left in these preparations. For measurements, monomers and trimers were diluted in a medium containing 20 mM HEPES buffer at pH 7.7, 60% (v/v) glycerol to ensure a transparent sample at low temperatures and 0.03% (w/v) *n*-dodecyl-β-D-maltoside, whereas for aggregates no detergent was used.

2.2. Theoretical background of Stark spectroscopy

Stark spectroscopy monitors the spectral changes induced by an electric field in the optical absorption or emission spectra of a molecule (for a recent review about Stark spectroscopy and its applications see for instance Ref. [37]). Usually, a shift in the transition energy is observed, whose magnitude depends on the change in dipole moment and polarisability, $\Delta\vec{\mu}$ and $\Delta\tilde{\alpha}$ between the ground and excited states upon excitation. In a multichromophoric system, the value of $\Delta\vec{\mu}$ can differ from the value for the individual pigments if significant excitonic interactions are present. In the case of molecules with antiparallel orientations, $\Delta\vec{\mu}$ can for instance become zero for both excitonic transitions [21,38,39]. On the other hand, mixing of charge-transfer states with the excited states ($\pi \rightarrow \pi^*$ transition) can lead to an increase in $\Delta\vec{\mu}$ as compared to the monomeric case. Quantitatively, the absorption spectral changes experienced by randomly oriented and spatially fixed molecules in the presence of an electric field can be described with the equation [37,40,41]

$$\Delta A(\nu) = (f\vec{F}_{\text{ext}})^2 \left\{ A_\chi A(\nu) + \frac{B_\chi}{15hc}\nu\frac{\mathrm{d}}{\mathrm{d}\nu}\left[\frac{A(\nu)}{\nu}\right] + \frac{C_\chi}{30h^2c^2}\nu\frac{\mathrm{d}^2}{\mathrm{d}\nu^2}\left[\frac{A(\nu)}{\nu}\right]\right\} \quad (1)$$

In Eq. (1), $\vec{F}_{\text{ext}}$ is the externally applied electric field and f is the local-field correction factor, which takes into account the enhancement of the applied electric field at the site of the molecule due to the environment. The terms A_χ, B_χ and C_χ are dependent on the macroscopic angle χ between the polarization direction of the light and the electric field. Information about the change in polarizability and permanent dipole moment upon excitation can be extracted from B_χ and C_χ,

$$B_\chi = \frac{1}{2}\mathrm{Tr}(\Delta\tilde{\alpha})\left[5 + (3\cos^2\chi - 1)\cdot 3\left(\frac{\vec{p}\cdot\Delta\tilde{\alpha}\cdot\vec{p}}{\mathrm{Tr}(\Delta\tilde{\alpha})}\right) - 1\right] \quad (2)$$

$$C_\chi = |\Delta\vec{\mu}|^2[5 + (3\cos^2\chi - 1)\cdot(3\cos^2\zeta - 1)] \quad (3)$$

When χ is set to magic angle (54.7°), all angle dependencies vanish, and $\mathrm{Tr}(\Delta\tilde{\alpha})$ and $|\Delta\vec{\mu}|$ can be obtained in a direct way. A_χ yields information about the intensity (proportional to the square of the transition dipole moment) of the optical transition.

Two types of analysis based on a nonlinear least-squares fitting program of the absorption and Stark spectra were performed, both yielding similar results. First, both spectra were fitted simultaneously with (skewed) Gaussian absorption bands and their first and second derivatives (for the Stark spectrum), providing estimates of $|\Delta\vec{\mu}|$ and $\mathrm{Tr}(\Delta\tilde{\alpha})$ for each Gaussian function. Second, a simultaneous fit of the absorption and Stark spectra was performed in certain wavelength regions with a polynomial function (Bspline [39]) and its first and second derivatives. Because f is not known, all the estimated values of $|\Delta\vec{\mu}|$ and $\mathrm{Tr}(\Delta\tilde{\alpha})$ are given in terms of D/f and Å^3/f^2, respectively, where $1\,\mathrm{D} = 3.34 \times 10^{-36}$ C m and $1\ \text{Å}^3 = 1.113 \times 10^{-40}$ C m^2/V.

2.3. Stark setup

The Stark setup is described in detail in Ref. [42] and many aspects of the experimental methods can be found in Ref. [37]. In essence, the Stark cell consists of two indium tin oxide (ITO)-coated glass plates glued together with double-sided sticky tape, resulting in a cell with an optical pathlength of ~100 μm. Excitation was provided by a 150-W Xenon lamp (Oriel). Measurements were carried out at 77 K (Oxford cryostat, DN1704) with the sample immersed in liquid nitrogen. The Stark effect was detected by lock-in amplification at 2ω, with ω being the frequency of the modulated field applied to the sample, which was set to 310 Hz. Stark and absorption spectra were recorded simultaneously. Separate absorption spectra were obtained with the lock-in amplifier (EG&G Model 5210) locked to the frequency of a chopper at 312 Hz. The OD of the samples ranged from 0.3 to 0.6 at the Q_y absorption maximum and the Stark signal scaled quadratically (see Eq. (1)) with the applied electric field in the range 0.8–2.3×10^5 V/cm.

3. Results

3.1. Monomers

Fig. 1 shows the absorption spectrum of monomeric LHCII together with its first and second derivative as well as the Stark spectrum at 77 K recorded at $\chi = 54.7°$. The absorption spectrum exhibits clear peaks in the Q_y region at 677 nm (Chl *a*) and at 649.5 nm (Chl *b*), whereas Soret bands are broader with maxima at 437 nm (Chl *a*) and 472 nm (Chl *b*). The second derivative of the absorption reveals additional bands at 670, 662, 494, 486, 466 and 458 nm. It is worth noting that the Chl *a* absorption in the Q_y region is

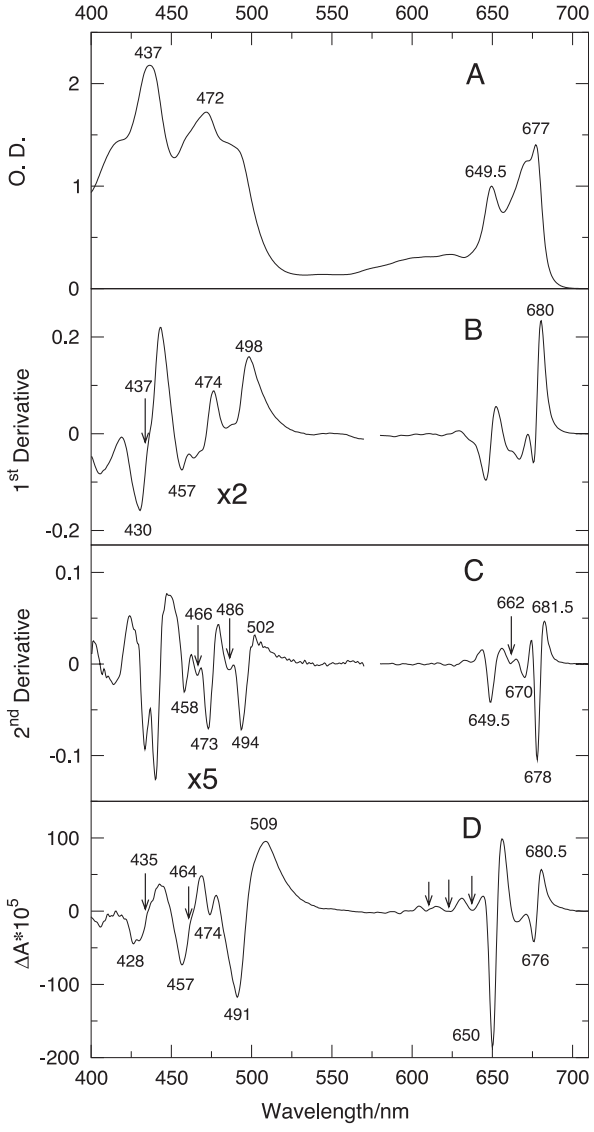

Fig. 1. (A) Absorption spectrum at 77 K of monomeric LHCII. (B) First derivative of the absorption of monomeric LHCII at 77 K. The Soret and carotenoid regions were enlarged by a factor of 2. (C) Second derivative of the absorption of monomeric LHCII at 77 K. The Soret and carotenoid regions were enlarged by a factor of 5. (D) Stark spectrum at 77 K of monomeric LHCII recorded at $\chi = 54.7°$. Spectra were normalized to OD = 1 at the Chl *b* peak (649.5 nm) and to a field strength of $F = 2.3 \times 10^5$ V/cm.

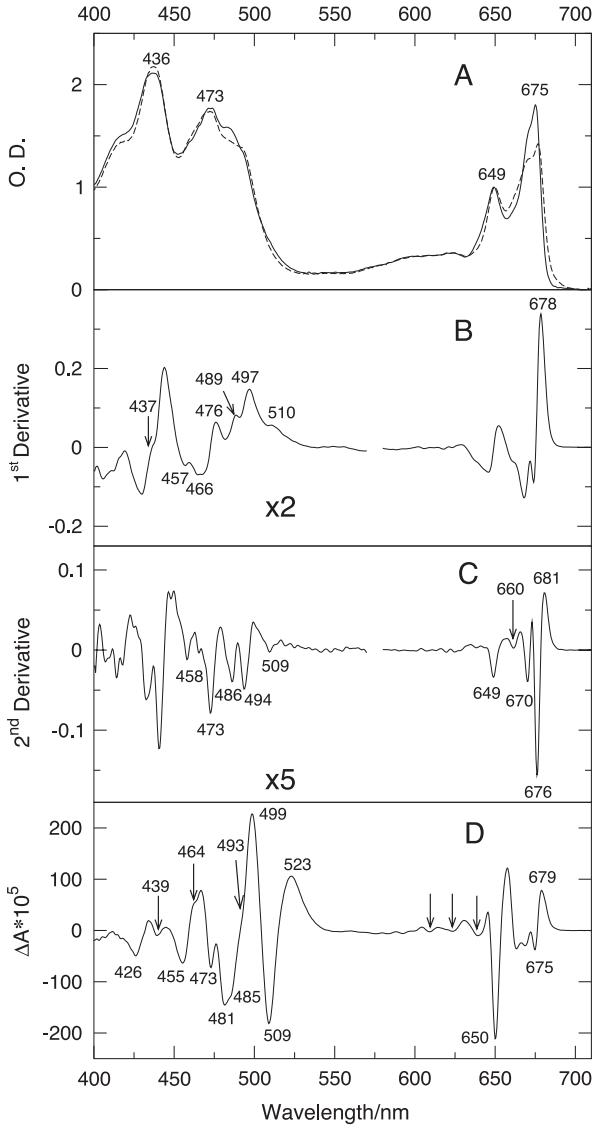

Fig. 2. (A) Absorption spectrum at 77 K of trimeric (continuous line) and monomeric (dashed line) LHCII. (B) First derivative of the absorption of trimeric LHCII at 77 K. The Soret and carotenoid regions were enlarged by a factor of 2. (C) Second derivative of the absorption of trimeric LHCII at 77 K. The Soret and carotenoid regions were enlarged by a factor of 5. (D) Stark spectrum at 77 K of trimeric LHCII recorded at $\chi = 54.7°$. Spectra were normalized to OD = 1 at the Chl *b* peak (649 nm) and to a field strength of $F = 2.3 \times 10^5$ V/cm.

broader than in the case of trimers (see below and Fig. 2), as was observed before [10,27], probably indicating a less rigid environment for the pigments in the monomers as compared to trimers. In addition, the main peak is ~ 2 nm shifted to the red (see below).

The Stark spectrum shows a complex structure due to the presence of many slightly different absorption bands. In the Chl *a* region (660–690 nm), the Stark signal can largely be accounted for by a linear combination of both the first and second derivatives of the absorption spectrum (see below). The Stark signal arising from the Chl *b* molecules resembles the shape of the second derivative spectrum. Several bands

are observed in the 560–630-nm region, but it is difficult to assign them unambiguously to the Q_x/vibrational transitions of Chl *a* and Chl *b* molecules.

The main features observed in the Soret and carotenoid region (400–550 nm) arise from both the Chl and carotenoid molecules. Lutein shows a large Stark signal characterized by a maximum at 509 nm and a minimum at 491 nm. The position of the minimum does not coincide with the minimum at 494 nm in the second derivative of the absorption spectrum (due to lutein), either because there is significant contribution from Chl *b* or neoxanthin to the Stark spectrum (although no identifiable additional spectral features can be detected, pointing in this direction) or because a significant difference polarizability for one or two luteins leads to considerable contribution from the first derivative spectrum of lutein. There are two additional pronounced negative bands at 457 and 428 nm, which at first sight seem to be the higher vibronic counterparts (S_2 $0 \rightarrow 1$ and S_2 $0 \rightarrow 2$ transitions) of the negative lutein peak at 491 nm (S_2 $0 \rightarrow 0$ transition). However, based on the spacing between these bands in the absorption spectrum of lutein (see, e.g. Ref. [34]), one would expect them to be located at 461 and 438 nm (positions estimated with respect to the minimum at 491 nm). If the 457 and 428 bands are indeed due to lutein, the contribution of the difference polarizability for these bands should be significantly larger than the contribution from the difference dipole moment, leading to more first derivative character of the Stark spectrum when compared to the band at 491 nm (S_2 $0 \rightarrow 0$ transition). Alternatively, the 428 and 457 bands are due to neoxanthin. Based on the position of the neoxanthin absorption maximum at 486 nm (S_2 $0 \rightarrow 0$ transition) and the spacing between the vibronic bands (see, e.g. Ref. [34]), one expects the vibronic absorption bands to be located at 456 and 430 nm, close to the minima in the Stark spectrum. It is somewhat surprising that no clear negative neoxanthin peak at 486 nm can be discerned, which could be due to the strong overlap with the broad 491-nm lutein component. Indeed, the latter band is asymmetric on the short-wavelength side (Fig. 1D). Finally, the negative peak at 474 nm should be ascribed to Chl *b*. In Table 1 the most likely assignments for lutein, neoxanthin and Chl *b* in the Soret-carotenoid region of monomeric LHCII are summarized.

Table 1
Assignment of the most relevant bands in the Soret and Carotenoid region for monomers and trimers of LHCII based on the Stark and absorption spectrum[a]

Monomers		Trimers	
Molecule	Bands	Molecule	Bands
–	–	*Red* Lut	509, 481 and 456
Lut	494, 466 and 435	*Blue* Lut	494, 464 and 439
Neo	486, 457 and 428	Neo	486, 455 and 426
Chl *b*	474 and 486	Chl *b*	473 and 486

[a] Due to the strong overlap of absorption bands below 475 nm, the assignment of the exact position for every band is less accurate.

3.2. Trimers

The absorption of trimeric LHCII together with its first and second derivative as well as the Stark spectrum at 77 K recorded at $\chi = 54.7°$ are plotted in Fig. 2. For comparison, the monomeric absorption spectrum is also shown. The peaks in the Q_y region are located at 675 and 649 nm, which correspond to Chl *a* and Chl *b*, respectively. In the Soret and carotenoid region similar peaks and shoulders are present as in the case of monomers. However, some striking differences can also be observed. In the red part (504–530 nm) of the carotenoid region, trimers of LHCII show the presence of a new band around 510 nm, as was previously observed [12]. From Raman experiments on trimeric LHCII it was concluded that the appearance of this band corresponds to a red shift of the absorption of one lutein from ~ 494 to ~ 510 nm [5,34], which was also corroborated by Caffarri et al. [7]. The absorption of trimeric LHCII also differs from that of monomeric LHCII in the region below 500 nm, which can largely be explained by the red shift of the lutein molecule. Inspection of the second derivative of the absorption of LHCII trimers similarly reveals the appearance of a new band at 509 nm.

The Stark spectrum of trimers shows a positive peak in the Q_y region of Chl *a* at 679 nm. As in the case of monomers, the shape of the Stark spectrum for the Chl *a* signal can largely be explained by a linear combination of the first and second derivatives of the absorption spectrum, whereas the signal in the Chl *b* spectral region looks more like the second derivative of the absorption spectrum. The new absorption band that appears at 509 nm upon trimerization shows a remarkably strong Stark signal, with two positive peaks at 523 and 499 nm and a minimum at 509 nm. Because the absorption maximum at 509 nm of the new band coincides with the minimum in the Stark spectrum, it can be concluded that for the lutein absorbing at this wavelength a large difference in dipole moment exists between ground and excited state. The Stark signal of the lutein peaking at 494 nm is partly buried by the intense signal from the lutein at 509 nm and other bands peaking more to the blue. Only a small dip can be observed at ~ 493 nm, close to the minimum in the absorption second derivative spectrum, indicating a dipole difference for the corresponding lutein as well, although significantly smaller than for the 509-nm lutein. A clear Stark minimum is present at 485 nm, probably due to a signal arising from neoxanthin and/or Chl *b* [5,12,34,43,44]. The pronounced minimum at 481 nm, which is absent in the monomer Stark spectrum, is attributed to the S_2 $(0 \rightarrow 1)$ transition of the red-most lutein. The S_2 $(0 \rightarrow 1)$ transition of the blue (i.e. absorbing at 494 nm) lutein probably is responsible for the dip at 464 nm in the Stark spectrum, in close correspondence with the assignment of Ruban et al. [34] stating that this lutein absorbs at 466 nm. The minima at 426 and 455 are most likely due to neoxanthin. The 439 nm minimum is likely to correspond to the blue lutein and

to Chl *a*, and the 473 nm feature to Chl *b*. Note that the assignment of the features below 473 nm is more speculative than the assignment of the other bands in the Soret and carotenoid region due to the strong overlap of multiple absorption bands with different Stark signals. We show in Table 1 the most probable assignments for lutein, neoxanthin and Chl *b* in the Soret-carotenoid spectral region of LHCII trimers.

3.3. Aggregates

Fig. 3 shows the 77 K absorption and Stark spectrum of LHCII aggregates, the latter being recorded at $\chi = 54.7°$. The absorption spectrum is partially distorted and flattened due to light scattering and sieving effects (see, e.g. Razi Naqvi et al. [30]). The absorption and Stark spectra of small aggregates of LHCII in the Q_y region are shown for comparison (dashed line). It is remarkable how similar the peak positions are in the Stark spectra of trimers and aggregates (Fig. 3B), most of them differing at most 1 nm. This is line with the conclusion by Razi Naqvi et al. [30] that most of the "real" absorption spectrum is not really distorted, the observed differences are largely due to scattering and the sieve effect. Similarly, Pieper et al. [28] and Ruban et al. [11] showed that aggregation has only little effect on the lowest electronic levels of the isolated trimer, with the exception of a slight red shift of ~ 2 nm for some spectral subbands. Stark features in regions of low absorption appear to be more intense for aggregates, largely due (if not completely) to the sieve effect, which is lower in these regions. The most pronounced "real" difference is the red shift of the positive Stark feature in the Chl *a* region from 679 to 683 nm.

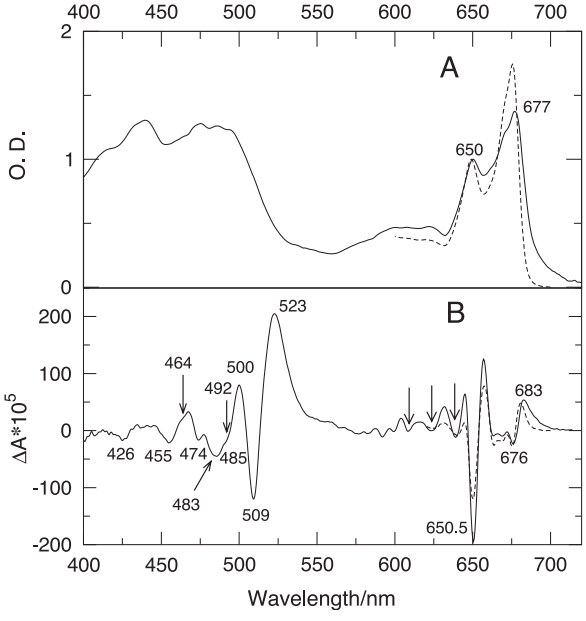

Fig. 3. (A) Absorption spectrum at 77 K of aggregated LHCII under light-scattering conditions (solid line) and of small aggregates of LHCII in the Q_y region (dashed line). (B) Stark spectrum at 77 K of aggregated LHCII recorded at $\chi = 54.7°$ under light-scattering conditions (solid line) and of small aggregates in the Q_y region (dashed line). Spectra were normalized to OD = 1 at the Chl *b* peak (650 nm) and to a field strength of $F = 2.3 \times 10^5$ V/cm. Note that, due to scattering and sieving effects, Stark features in regions of low absorption appear to be more intense for aggregates (see text for details).

It is worth noting that the pronounced minimum in the Stark spectrum due to Chl *b* is always located at ~ 650 nm, independent of the state of oligomerisation of LHCII. In the case of Krawczyk et al. [35], the minimum was located at ~ 654 nm, that is, their Stark spectrum was ~ 4 nm red shifted with respect to the absorption, which showed a maximum located at 650 due to the Q_y absorption band of the Chl *b* molecules.

4. Discussion

4.1. Chl a Q_y region

The Stark effect in the Chl *a* Q_y region shows an overall similarity between monomers, trimers and aggregates, although there are some specific differences. For instance, monomers and aggregates exhibit a red shift of the main Chl *a* positive signal with respect to trimers, which can be up to 4 nm for aggregates of LHCII.

Figs. 4 and 5 show the fit in the Q_y region using Gaussian functions for both absorption and Stark spectra of monomers and trimers, respectively. Four bands in both samples were required to account for the Chl *a* absorption and Stark effect (660–690 nm spectral region). For clarity of the figure only the contributions of the bands located at ~ 676 and ~ 670 nm to the fit of the Stark spectrum are shown. We do not assign much significance to the band located at 688.5 nm in monomers because its relative area is very small.

In Table 2 the values for $|\Delta\vec{\mu}|$ and $\mathrm{Tr}(\Delta\tilde{\alpha})$ obtained from the fit for the different bands are summarized for both complexes. In both cases, the bands associated to the Chl *a* chromophores exhibit values close to 0.6 D/*f* for the change in dipole moment and between 40 and 70 $Å^3/f^2$ for the change in polarizability. The largest changes in polarizability are found for the red part of the spectrum of the monomers. The $|\Delta\vec{\mu}|$ values for the Chl *a* spectral forms absorbing to the red of the main peak in trimers (676 and 679 nm) are in agreement with the value reported by Rätsep et al. [45] of 0.63 D/*f* for the lowest energy state in trimeric LHCII located at 680 nm. In contrast, they are lower than the ones reported by Krawczyk et al. [35], who found $|\Delta\vec{\mu}|$ to be 1.0 D/*f*. Their fits were, however, less satisfactory than in our case: significantly higher deviations were observed, probably because of scattering and sieving effects and the shift of ~ 4 nm in the Stark spectrum with respect to the absorption. In Fig. 6, a simultaneous fit of the absorption and Stark in the Chl *a* Q_y region with a polynomial function (Bspline [39]) and its derivatives is shown for monomers, trimers and small

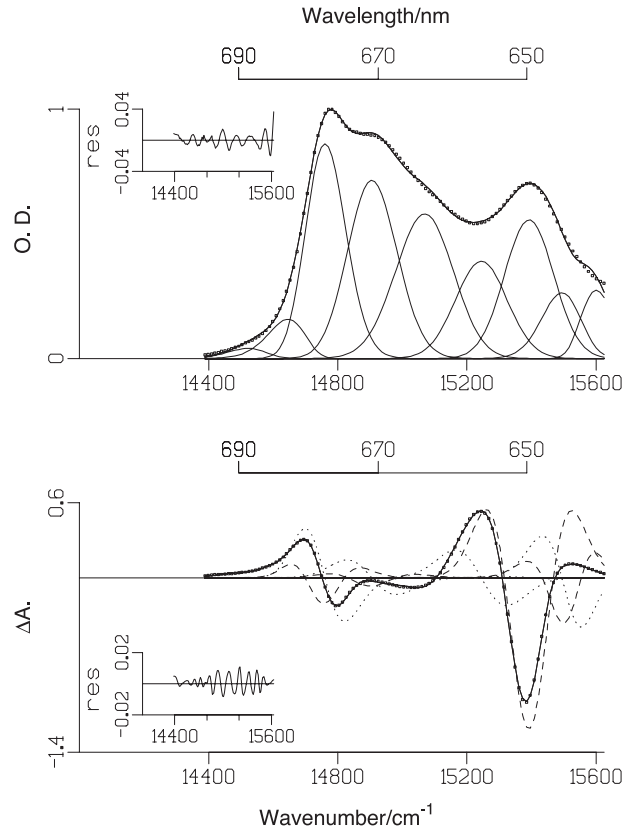

Fig. 4. Simultaneous fit of the 77 K absorption and Stark spectra of monomeric LHCII (Q_y region) recorded at $\chi = 54.7°$ with Gaussian functions for the absorption (top), and the first (dotted lines) and second (dashed lines) derivatives of these functions for the Stark spectrum (bottom). For clarity, only the derivatives of the Gaussian functions located at 677.5, 671, 656.5, 650 and 645.5 nm are shown. The insets show the residuals from the fit.

aggregates (Fig. 3, dashed line). The results of the fit, which are presented in Table 3, are similar to the values in Table 2, and support the conclusion that the electro-optical parameters corresponding to the Chl *a* molecules in LHCII are $|\Delta\vec{\mu}| \sim 0.6$ D/f and $\mathrm{Tr}(\Delta\tilde{\alpha}) \sim 55$ Å^3/f^2 over the whole Chl *a* Q_y region.

It is of interest to compare the obtained values with those of monomeric Chl *a*. Several values have been reported for the change in dipole moment and polarizability between the ground and excited states for monomeric Chl *a* [45–47]. The most recent $|\Delta\vec{\mu}|$ value was reported by Rätsep et al. [45] from Stark hole-burning effect of Chl *a* deposited in a poly(vinyl butyral) (PVB) film. The value found was 0.52 D/*f*. The correlation found between $\Delta\vec{\mu}$ and $\Delta\tilde{\alpha}$ on spectral holes in PVB films from Stark hole-burning measurements is given by the equation [46]

$$\Delta\vec{\mu} = -0.04 + 8.8\Delta\tilde{\alpha}/\mathrm{MW} \quad (4)$$

where MW describes the molecular weight of the dopant. Then, for a $|\Delta\vec{\mu}|$ value of 0.52 D/*f*, $\Delta\tilde{\alpha} = 20$ Å^3/f^2, which is of the same order of magnitude as our obtained value $\mathrm{Tr}(\Delta\tilde{\alpha}) \sim 55$ Å^3/f^2 for Chl *a* bound to LHCII (one should keep in mind that the reported in this work is generally defined as $1/3\ \mathrm{Tr}(\Delta\tilde{\alpha}) = \Delta\tilde{\alpha}$).

The fact that $|\Delta\vec{\mu}|$ and $\mathrm{Tr}(\Delta\tilde{\alpha})$ for Chl *a* bound to LHCII are very similar to the values for monomeric Chl *a* implies that the Chl *a* molecules in LHCII behave like monomeric weakly coupled Chl *a*, in agreement with previous studies [19,24,25]. Rätsep et al. [45] also reached the same conclusion. Strong excitonic interactions, which can lead to a significant delocalization of excitations over many pigments and to a decrease in $|\Delta\vec{\mu}|$, are apparently absent.

4.2. Aggregates exhibit no charge-transfer state

In a hole-burning study on aggregates of LHCII, Pieper et al. [28] were unable to burn holes upon selective excitation above 682 nm. They attributed this to the presence of (a) red-shifted of state(s) with charge-transfer character. They argued that these states, which hardly fluoresce, might function as trap states for excitations, thereby explaining the decrease of fluorescence yield upon

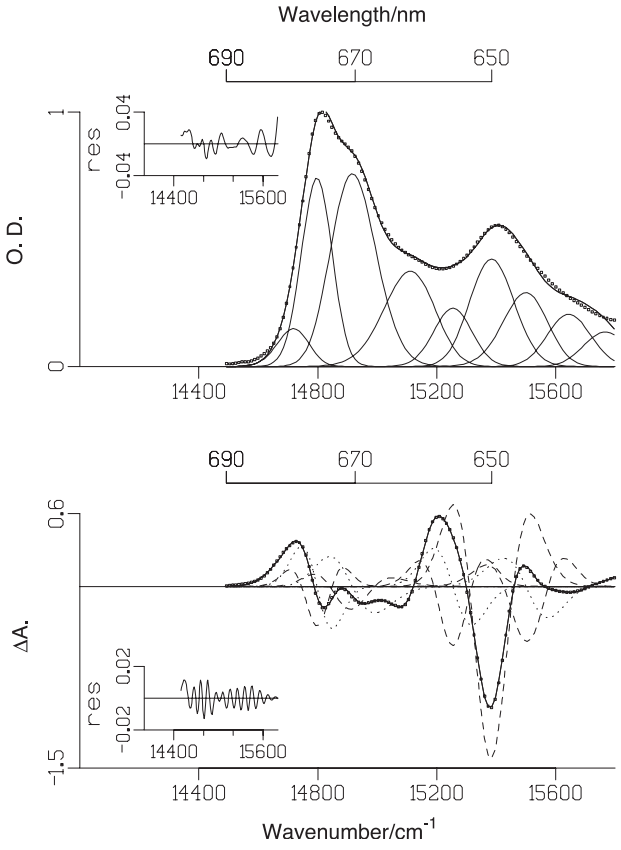

Fig. 5. Simultaneous fit of the 77 K absorption and Stark spectra of trimeric LHCII (Q_y region) recorded at $\chi = 54.7°$ with Gaussian functions for the absorption (top), and the first (dotted lines) and second (dashed lines) derivatives of these functions for the Stark spectrum (bottom). For simplicity of the figure, only the derivatives of the Gaussian functions with maxima at 676, 670.5, 655.5, 650 and 645 nm are depicted. The insets show the residuals from the fit.

Table 2
Stark parameters for monomeric and trimeric LHCII in the Q_y region

Monomers				Trimers				Krawczyk et al. [35]			
Gaussian band	Relative area (%)	$\lvert\Delta\vec{\mu}\rvert$ (D/f) (± 10%)	Tr($\Delta\tilde{\alpha}$) (Å^3/f^2) (± 10%)	Gaussian band	Relative area (%)	$\lvert\Delta\vec{\mu}\rvert$ (D/f) (± 10%)	Tr($\Delta\tilde{\alpha}$) (Å^3/f^2) (± 10%)	Gaussian band	Relative area (%)	$\lvert\Delta\vec{\mu}\rvert$ (D/f)	$\Delta\tilde{\alpha}$ (Å^3/f^2)
(688.5)	1.2	–	–	–	–	–	–	(695)	–	–	–
683.0	3.1	0.6	80	679.5	4.1	0.6	65	685.0	4.3	–	–
677.5	20.3	0.5	70	676.0	16.9	0.6	56	678.0	24.9	1.0	–[a]
671.0	23.1	0.4	40	670.5	27.1	0.7	54	671.3	16.3	1.3	–[a]
663.5	19.3	0.6	30	661.5	15.7	1.3	–	665.0	8.3	2.2	–
–	–	–	–	–	–	–	–	662.0	11.0	1.7	–
656.5	12.2	–	95	655.5	5.6	1.5	230	656.0	10.3	2.3	70
650.0	16.2	1.9	–	650.0	14.5	2.3	–	649.0	16.0	1.1	–
645.5	5.8	1.2	180	645.0	9.6	1.8	180	642.2	5.9	1.5	–
(641.0)	–	–	–	639.0	6.4	1.2	–	639.5	3.0	1.7	–
–	–	–	–	(634.0)	–	–	–	621.0	–	–	–

[a] In Ref. [35] $\Delta\tilde{\alpha}$ was estimated from the first and second derivatives of the absorption spectrum yielding a value of 8 ± 2 Å^3/f^2.

aggregation. In Table 3, the values for $\lvert\Delta\vec{\mu}\rvert$ and Tr($\Delta\tilde{\alpha}$) for aggregates of LHCII in the Chl *a* Q_y region are shown. Within experimental error they are the same as for monomeric uncoupled Chl *a* (see discussion above). This excludes the possibility that the red Chl *a* molecules in aggregates have a charge-transfer state, which would be characterized by a large change in dipole moment [21], as found for instance in the reaction center of photosynthetic bacteria [48]. A possible explanation for the inability to burn a hole in the red-most part of the absorption spectrum could be that the absorption spectrum is distorted due to scattering and sieving effects, leading to an apparent increase of the red-most absorption [29,30] (see above). It should be noted that for none of the Chl *a* bands high $\Delta\vec{\mu}$ values are found, indicating weak electron–phonon interaction, i.e. low values for the Huang–Rhys factor S [45]. This is in perfect agreement with previous observations for LHCII [24,25].

4.3. Chl b Q_y region

The Stark effect in the Chl *b* Q_y region (635–660 nm) for monomers and trimers is very similar and looks mostly like the second derivative of the absorption. Four (monomers) and five (trimers) bands were required to fit the absorption and Stark signals in this spectral region (see Table 2 and Figs. 4 and 5). The width of the Gaussian bands ranges from 140 to 190 cm^{-1} and the bands become broader on the blue side when going from monomers to trimers (142 versus 176

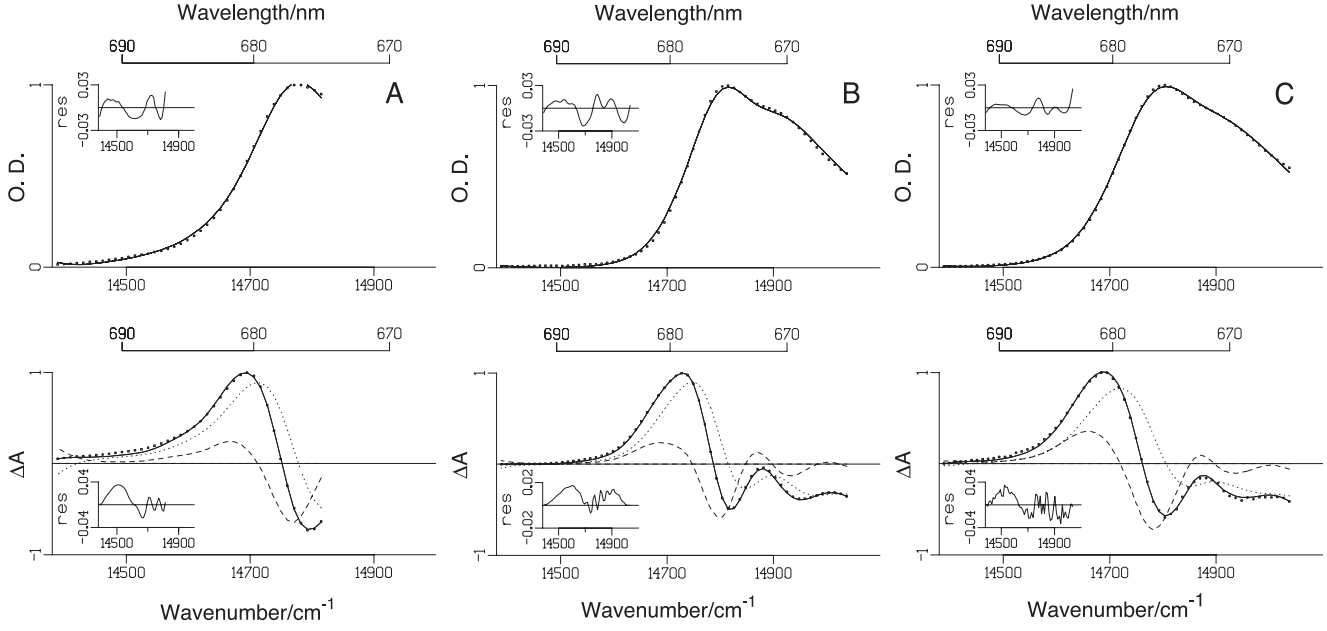

Fig. 6. Simultaneous fit of the 77 K absorption and Stark spectra of monomeric (A), trimeric (B) and aggregated (C) LHCII (Chl *a* Q_y region) recorded at $\chi = 54.7°$ with a polynomial function and its first (dotted lines) and second (dashed lines) derivatives. The aggregated sample corresponds to the one shown in Fig. 3, dashed line. The fitted spectral region ranges from 695 to 665 nm except for the monomeric sample, where a satisfactory fit could not be obtained when wavelengths below 675 nm were included. The residuals from the fits are included in the insets of every figure.

Table 3
Stark parameters of Chl *a* in various oligomeric forms of LHCII estimated using a fit with a polynomial function, and its first and second derivatives[a]

State of oligomerization	$\lvert\Delta\vec{\mu}\rvert$ (D/*f*)	Tr($\Delta\tilde{\alpha}$) (Å^3/*f*^{2})
Monomers	0.59 ± 0.06	58 ± 6
Trimers	0.58 ± 0.06	58 ± 6
Aggregates	0.63 ± 0.06	40 ± 6

[a] The fitted spectral region ranged from 695 to 665 nm except for monomers, where a satisfactory fit could not be obtained when wavelengths below 675 nm were included.

cm^{-1}), in agreement with the qualitative behaviour observed in the absorption.

There is an enhancement in $\lvert\Delta\vec{\mu}\rvert$ for the main band at ~650 nm in trimers comparing to monomers and the values are higher than the values expected for monomeric Chl *b* (1.4–1.6 D/*f* [35]). In the analysis done by Krawczyk et al. [35] (see Table 2), the band located at 656.0 nm is the one with a relatively high $\lvert\Delta\vec{\mu}\rvert$ (2.3 D/*f*), whereas the band at 649 possesses a $\lvert\Delta\vec{\mu}\rvert$, which has half the value of the former one. This can be explained by the fact that the pronounced minimum in the Stark spectrum of Krawczyk et al. due to Chl *b* was located at ~654 nm in Ref. [35], i.e. 4 nm to the red of the absorption spectrum, whereas in our case the values differ less than one nanometer. This rather large value for the difference dipole moment between the ground and excited states both for monomers (1.9 D/*f*) and trimers (2.3 D/*f*) is three or four times higher than for the Chl *a* absorption bands around 675 nm, whereas for isolated chlorophylls this ratio is approximately 1.5 [35]. We speculate that this large value is due to the interaction of some Chls *b* with neoxanthin. According to Croce et al. [17], the neoxanthin binding site is located between the helix C and helix A/B domains, in close contact with chlorophylls *b*5 and *b*6 in the model proposed by Kühlbrandt et al. [15]. Strong electrostatic interactions and/or partial electron density overlap between Chl *b* molecules and neoxanthin might produce an increase for $\lvert\Delta\vec{\mu}\rvert$ with respect to the expected monomeric Chl *b* value. Moreover, it is known that the absence of neoxanthin in reconstituted LHCII also leads to a significant change in (polarized) absorption around 650 nm, where the neoxanthin itself is not expected to be absorbing (Croce et al. [17]).

4.4. Red-most carotenoid bands

The simultaneous fit of the absorption and Stark effect in the red-most part of the carotenoid region for monomers and trimers are plotted in Figs. 7 and 8, respectively. In both cases bands at ca. 494 nm (Lut) and 485 nm (Neo-Chl *b*) were needed with their fwhm ranging from ~400 to ~600 cm^{-1}. The monomer Stark spectrum shows a rather complicated shape on the red edge, which cannot be satisfactorily fit with a combination of the first and second derivatives of a single absorption band. This indicates that the Stark effect in this region arises from more than one pool of lutein molecules absorbing at different wavelengths, as can also be seen in Table 4. However, Ruban et al. [5] reported that both luteins in monomeric LHCII absorb at around 495 nm, although slight differences in their protein environments give rise to a broadening of the corresponding absorption band. The values reported in Table 4 for each of the Gaussian bands in monomeric LHCII are of the same order of magnitude as those reported for carotenoids in glassy solvents [49].

Trimers exhibit an additional broad band at 509 nm with an fwhm of 715 cm^{-1} (18 nm), like the one reported by Ruban et al. [5]. Also T – S measurements on trimeric LHCII revealed that the 525 nm T – S band, corresponding to a ground state absorption band close to 510 nm, is broader than the T – S band located at 507 nm (associated with the 494-nm band in absorption) [12]. The fitted area of the 509-nm band is approximately one third of that of the 494-nm band, suggesting that both bands do not simply correspond to one xanthophyll molecule per monomeric subunit, although the Raman spectrum indicates that both of them should be ascribed to lutein [34]. This band at 509 nm also shows a threefold increase in $\lvert\Delta\vec{\mu}\rvert$ (~15 D/*f*) with

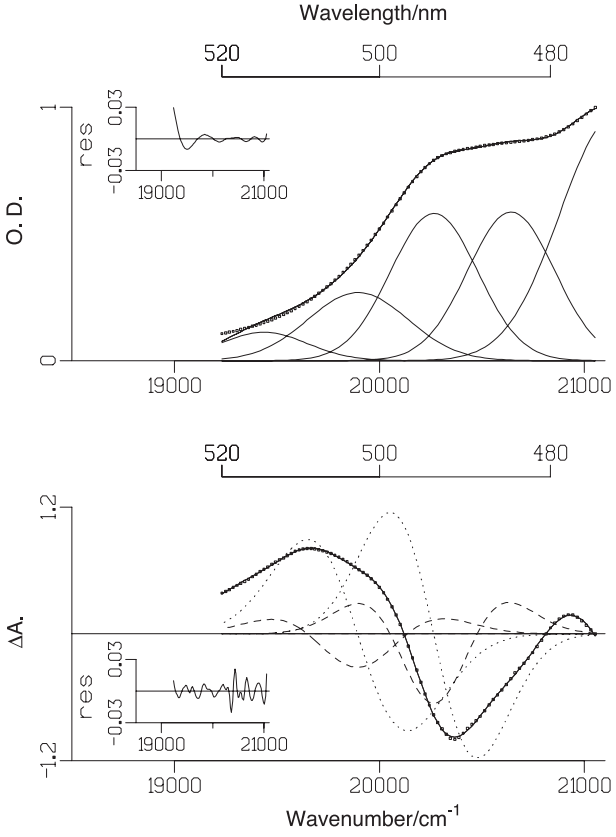

Fig. 7. Simultaneous fit of the 77 K absorption and Stark spectra of monomeric LHCII (carotenoid region) recorded at $\chi = 54.7°$ with Gaussian functions for the absorption (top), and the first (dotted lines) and second (dashed lines) derivatives of these functions for the Stark spectrum (bottom). For clarity, only the derivatives of the Gaussian functions located at 502.5 and 493.5 nm are shown. The residuals from the fit are included in the insets.

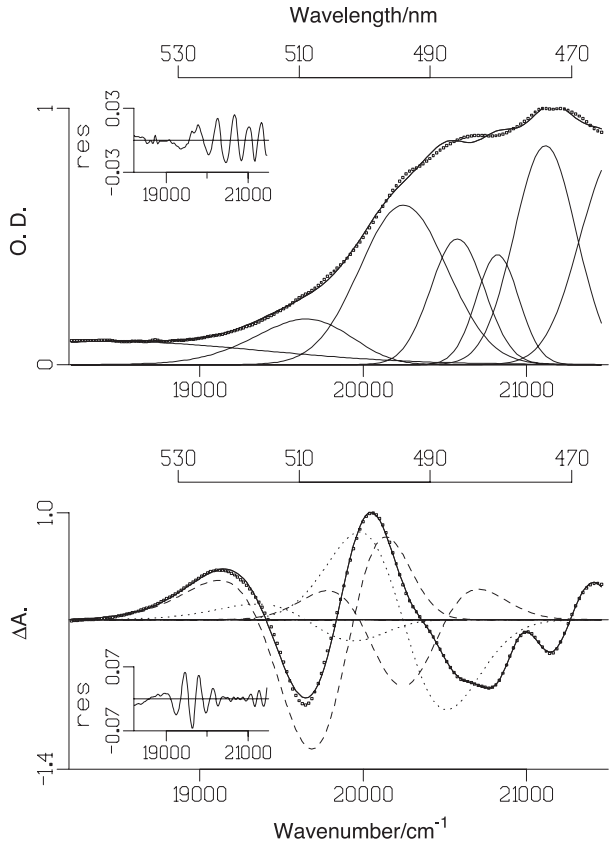

Fig. 8. Simultaneous fit of the 77 K absorption and Stark spectra of trimeric LHCII (carotenoid region) recorded at $\chi = 54.7°$ with Gaussian functions for the absorption (top), and the first (dotted lines) and second (dashed lines) derivatives of these functions for the Stark spectrum (bottom). For simplicity of the figure, only the derivatives of the red most Gaussian functions are depicted. The residuals from the fit are included in the insets.

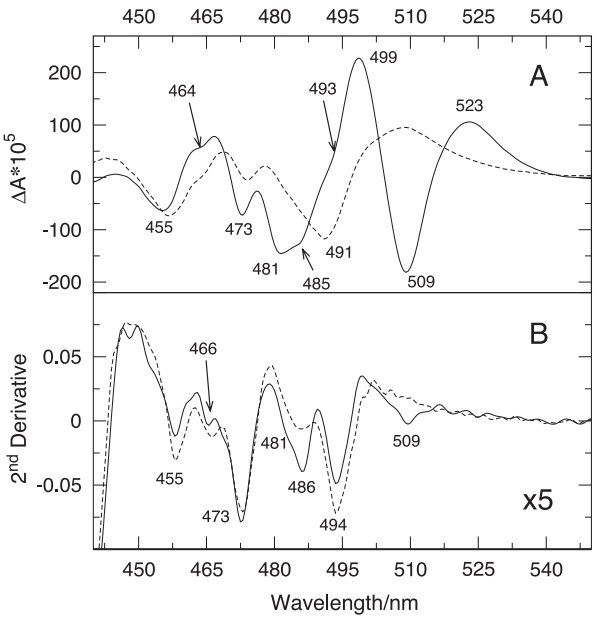

Fig. 9. (A) Stark spectrum at 77 K of monomeric (dashed) and trimeric (solid) LHCII recorded at $\chi = 54.7°$. Spectra were normalized to OD = 1 at the Chl *b* (649 nm) peak and to a field strength of $F = 2.3 \times 10^5$ V/cm. (B) Second derivative of the absorption of monomeric (dashed) and trimeric (solid) LHCII at 77 K. Both derivatives were enlarged by a factor of 5.

respect to glassy solvents. Most strikingly, the electro-optical properties of the red-most carotenoid band are very sensitive to the aggregation state of LHCII, but it remains somewhat puzzling to account for the observed differences in electro-optical properties of these two absorption bands—494 and 509 nm—corresponding to the lutein molecules. Fig. 9 shows both Stark spectra and second derivatives of the absorption spectra for the red-most carotenoids in monomers and trimers. It can readily be observed that the 509-nm band for trimers (and aggregates) exhibits a huge Stark signal.

In order to explain the big difference in $|\Delta\vec{\mu}|$ for the two lutein bands, the electric field experienced by the lutein molecules should be significantly larger in trimers than in monomers. It is known [37,39] that a large electric field can transform a change in polarizability $\Delta\tilde{\alpha}$ into a difference in dipole moment $\Delta\vec{\mu}$ according to: $\Delta\vec{\mu} = \vec{E} \cdot \Delta\tilde{\alpha}$. Monomerization of LHCII trimers has recently been shown to be induced by light illumination [50]. This process leads simultaneously to the disappearance of the band located at 509 nm due to lutein and to the release of up to 2.5 Mg ions per trimer [50]. It is tempting to speculate that the presence of a Mg ion in the neighborhood of one of the lutein molecules enhances the electric field around this xanthophyll, thereby explaining the large value of $|\Delta\vec{\mu}|$ for the 509-nm band (and probably also the large red shift of this

Table 4
Stark parameters for monomeric and trimeric LHCII in the red part of the carotenoid region

Monomers				Trimers			
Gaussian band	Relative area (%)	$\lvert\Delta\vec{\mu}\rvert$ (D/*f*) (± 15%)	Tr($\Delta\tilde{\alpha}$) (Å^3/*f*$^{-2}$) (± 15%)	Gaussian band	Relative area (%)	$\lvert\Delta\vec{\mu}\rvert$ (D/*f*) (± 15%)	Tr($\Delta\tilde{\alpha}$) (Å^3/*f*$^{-2}$) (± 15%)
–	–	–	–	(542.0)[a]	–	–	–
514.5	–	–	630	–	–	–	–
502.5	21.3	3.5	1170	509.0	11.2	14.6	640
493.5	39.5	3.0	610	493.5	33.0	5.5	1000
484.5	39.2	2.3	250	486.0	13.9	3.0	740
–	–	–	–	480.5	11.2	2.5	250
475.0	–	1.9	230	473.5	30.7	2.5	135

[a] This Gaussian band was included to minimize the error due to the baseline and contributions from the Chl molecules. Its Stark parameters were set to zero.

absorption band). Note that the 509-nm band is presumably due to lutein 2 [31]. From Raman studies, it is also known that the 510-nm lutein is geometrically a very asymmetric molecule [34]. This change in geometry for some of the lutein molecules which might also be caused by the presence of the Mg ions, can lead to a redistribution of charges on the luteins favoring a high value for $|\Delta\vec{\mu}|$.

The fact that only up to 2.5 Mg ions per trimer are released (depending on the light intensity) [50] might also explain the presence of a small absorption band at higher wavelengths than 494 nm in monomers as well. If a fraction of Mg ions is present in LHCII monomers, some lutein absorption will occur above 494 nm. The absorption band associated to these lutein molecules might not be noticeable in conventional absorption, but might easily show up in the field-on minus field-off absorbance difference spectrum.

It remains unclear why the 509-nm lutein band seems to be less intense than the 494-nm band. In general, the most straightforward explanation for such a difference is the presence of strong excitonic interactions, either between the two lutein molecules or between lutein and chlorophyll. A rough dipole–dipole calculation indicates that the coupling strength between the two lutein molecules is in the order of 80 cm^{-1}, which is rather small when compared to the widths of the bands. Therefore, excitonic interactions cannot explain such a pronounced difference in intensity (Somsen et al. [51]). Moreover, both the lutein band at 494 nm and the Chl *a* bands have electro-optical properties that are very similar to those of the monomeric pigments, thereby arguing against such an explanation. Alternatively, the strong coupling with Chl molecules might lead to hyper- or hypochromic effects for the luteins. The size of the interactions would have to differ considerably for both luteins in order to explain the apparent difference in intensity. However, femtosecond transient absorption measurements do not indicate significant differences [44,52]. Exciton energy transfer times from both luteins to Chl *a* are very similar, indicating similar coupling strengths. Therefore, we conclude that excitonic interactions are not responsible for the significant differences in intensity of the two lutein bands, and only heterogeneity between trimers possibly due to the presence or absence of Mg ions [50] might account for the difference in dipole strength of the lutein bands.

We conclude from the Stark spectrum that the band at 485 nm is not only due to neoxanthin but also to Chl *b* molecules. The corresponding values of the difference dipole and difference polarizability are substantially lower than for the lutein bands, confirming the assignment to both neoxanthin and Chl *b*, the latter having a much smaller electro-optical response. This dual assignment agrees nicely with the conclusions drawn from femtosecond pump-probe experiments [43,44].

The band at 481 nm can safely be attributed to the red lutein absorbing at 509 nm because it presents a relatively strong Stark effect like the 509 band, which is absent in the Stark spectrum of LHCII monomers. However, the changes in dipole moment and polarizability upon excitation are more difficult to determine due to the overlap of many different transitions. The most likely origin of the other bands that are present to the blue of the 481-nm band have already been discussed above (see also Table 1).

5. Conclusions

Virtually all the Chl *a* absorption bands in the Q_y region have electro-optical properties that are very similar to those of monomeric Chl *a*, which argues against strong exciton delocalization over the Chl *a* molecules in LHCII.

We did not observe charge-transfer character for any of the Chl *a* Q_y absorption bands for LHCII aggregates, in particular not for the red-most bands, arguing against the possibility that charge-transfer states are responsible for the fluorescence quenching for LHCII aggregates [28].

The main Chl *b* absorption band in the Q_y region has electro-optical properties that are more pronounced than for monomeric Chl *b*, which is tentatively explained by strong interaction between some Chls *b* and neoxanthin.

The Stark measurements confirm the presence of a lutein absorption band around 510 nm in trimers and aggregates, and this band has considerably different optical properties (maximum, width, $|\Delta\vec{\mu}|, \Delta\tilde{\alpha}$) than the 494-nm lutein band.

Finally, the 486-nm band is due to both neoxanthin and chlorophyll *b*.

Acknowledgements

Visit(s) of A.V. Ruban to Amsterdam were supported by the European Union (Improving Human Potential Contract no. HPRI-CT-1999-00064). We thank Prof. G. Garab for valuable discussions.

References

[1] W. Kühlbrandt, D.N. Wang, Three-dimensional structure of plant light-harvesting complex determined by electron crystallography, Nature 350 (1991) 130–134.
[2] R. van Grondelle, J.P. Dekker, T. Gillbro, V. Sundström, Energy transfer and trapping in photosynthesis, Biochim. Biophys. Acta 1187 (1994) 1–65.
[3] S. Jansson, The light-harvesting chlorophyll *a*/*b*-binding proteins, Biochim. Biophys. Acta 1184 (1994) 1–19.
[4] A.V. Ruban, P.J. Lee, M. Wentworth, A.J. Young, P. Horton, Determination of the stoichiometry and strength of binding of xanthophylls to the photosystem II light-harvesting complexes, J. Biol. Chem. 274 (1999) 10458–10465.
[5] A.V. Ruban, A.A. Pascal, B. Robert, P. Horton, Configuration and dynamics of xanthophylls in light-harvesting antennae of higher plants, J. Biol. Chem. 276 (2001) 24862–24870.
[6] R. Croce, S. Weiss, R. Bassi, Carotenoid-binding Sites of the Major Light-harvesting Complex II of Higher Plants, J. Biol. Chem. 274 (1999) 29613–29623.
[7] S. Caffarri, R. Croce, J. Breton, R. Bassi, The major antenna complex

of photosystem II has a xanthophyll binding site not involved in light harvesting, J. Biol. Chem. 276 (2001) 35924–35933.
[8] A.V. Ruban, P. Horton, Mechanism of ΔpH-dependent dissipation of absorbed excitation energy by photosynthetic membranes: I. Spectrosopic analysis of isolated light-harvesting complexes, Biochim. Biophys. Acta 1102 (1992) 30–38.
[9] K.-D. Irrgang, E.J. Boekema, J. Vater, G. Renger, Structural determination of the photosystem-II core complex from spinach, Eur. J. Biochem. 178 (1988) 209–217.
[10] S. Nussberger, J.P. Dekker, W. Kühlbrandt, B.M. van Bolhuis, R. van Grondelle, H. van Amerongen, Spectroscopic characterization of three different monomeric forms of the main chlorophyll *a*/*b* binding protein from chloroplast membranes, Biochemistry 33 (1994) 14775–14783.
[11] A.V. Ruban, F. Calkoen, S.L.S. Kwa, R. van Grondelle, P. Horton, J.P. Dekker, Characterisation of LHC II in the aggregated state by linear and circular dichroism spectroscopy, Biochim. Biophys. Acta 1321 (1997) 61–70.
[12] E.J.G. Peterman, C.C. Gradinaru, F. Calkoen, J.C. Borst, R. van Grondelle, H. van Amerongen, Xanthophylls in light-harvesting complex II of higher plants: light harvesting and triplet quenching, Biochemistry 36 (1997) 12208–12215.
[13] P.W. Hemelrijk, S.L.S. Kwa, R. van Grondelle, J.P. Dekker, Spectroscopic properties of LHC-II, the main light-harvesting chlorophyll *a*/*b* protein complex from chloroplast membranes, Biochim. Biophys. Acta 1098 (1992) 159–166.
[14] A.V. Ruban, D. Phillip, A.J. Young, P. Horton, Carotenoid-dependent oligomerization of the major chlorophyll *a*/*b* light harvesting complex of photosystem II of plants, Biochemistry 36 (1997) 7855–7859.
[15] W. Kühlbrandt, D.N. Wang, Y. Fujiyoshi, Atomic model of plant light-harvesting complex by electron crystallography, Nature 367 (1994) 614–621.
[16] S. Hobe, H. Niemeier, A. Bender, H. Paulsen, Carotenoid binding sites in LHCIIb-Relative affinities towards major xanthophylls of higher plants, Eur. J. Biochem. 267 (2000) 616–624;
E. Formaggio, G. Cinque, R. Bassi, Functional architecture of the major light-harvesting complex from higher plants, J. Mol. Biol. 314 (2001) 1157–1166.
[17] R. Croce, R. Remelli, C. Varotto, J. Breton, R. Bassi, The neoxanthin binding site of the major light harvesting complex (LHCII) from higher plants, FEBS Lett. 456 (1999) 1–6.
[18] H. van Amerongen, R. van Grondelle, Understanding the energy transfer function of LHCII, the major light-harvesting complex of green plants, J. Phys. Chem. B 105 (2001) 604–617.
[19] M.A. Palacios, F.L. de Weerd, J.A. Ihalainen, R. van Grondelle, H. van Amerongen, Superradiance and exciton (De)localization in light-harvesting complex II from green plants? J. Phys. Chem. B 106 (2002) 5782–5787.
[20] V. Novoderezhkin, J.M. Salverda, H. van Amerongen, R. van Grondelle, Exciton modeling of energy-transfer dynamics in the LHCII complex of higher plants: a redfield theory approach, J. Phys. Chem. B 107 (2003) 1893–1912.
[21] H. van Amerongen, L. Valkunas, R. van Grondelle, Photosynthetic Excitons, 1st ed., World Scientific, Singapore, 2000, Chaps. 2, 3 and 7.
[22] D. Gülen, R. van Grondelle, H. van Amerongen, Structural information of the light-harvesting complex II of green plants that can be deciphered from polarized absorption characteristics, J. Phys. Chem. B 101 (1997) 7256–7261.
[23] G. Zucchelli, F.M. Garlaschi, R.C. Jennings, Thermal broadening analysis of the light harvesting complex II absorption spectrum, Biochemistry 35 (1996) 16247–16254.
[24] E.J.G. Peterman, T. Pullerits, R. van Grondelle, H. van Amerongen, Electron–phonon coupling and vibronic fine structure of light-harvesting complex II of green plants: temperature dependent absorption and high-resolution flurescence spectroscopy, J. Phys. Chem. B 101 (1997) 4448–4457.
[25] J. Pieper, M. Rätsep, R. Jankowiak, K.-D. Irrgang, J. Voigt, G. Renger, G.J. Small, *Qy*-level structure and dynamics of solubilized light-harvesting complex II of green plants: pressure and hole burning studies, J. Phys. Chem. A 103 (1999) 2412–2421.
[26] H. van Amerongen, S.L.S. Kwa, B.M. van Bolhuis, R. van Grondelle, Polarized fluorescence and absorption of macroscopically aligned light harvesting complex II, Biophys. J. 67 (1994) 837–847.
[27] C.C. Gradinaru, S. Özdemir, D. Gülen, I.H.M. van Stokkum, R. van Grondelle, H. van Amerongen, The flow of excitation energy in LHCII monomers: implications for the structural model of the major plant antenna, Biophys. J. 75 (1998) 3064–3077.
[28] J. Pieper, K.-D. Irrgang, M. Rätsep, R. Jankowiak, Th. Schrötter, J. Voigt, G.J. Small, G. Renger, Effects of aggregation on trimeric light-harvesting complex II of green plants: a hole-burning study, J. Phys. Chem. A 103 (1999) 2422–2428.
[29] L.N.M. Duysens, The flattening of the absorption spectrum of suspensions, as compared to that of solutions, Biochim. Biophys. Acta 19 (1956) 1–12.
[30] K. Razi Naqvi, T.B. Melø, B. Bangar Raju, T. Jávorfi, G. Garab, Comparison of the absorption spectra of trimers and aggregates of chlorophyll *a*/*b* light-harvesting complex LHC II, Spectrochim. Acta, Part A 53 (1997) 1925–1936.
[31] S.S. Lampoura, V. Barzda, G.M. Owen, A.J. Hoff, H. van Amerongen, Aggregation of LHCII leads to a redistribution of the triplets over the central xanthophylls in LHCII, Biochemistry 41 (2002) 9139–9144.
[32] M. Wentworth, A.V. Ruban, P. Horton, Kinetic analysis of nonphotochemical quenching of chlorophyll fluorescence. 2. Isolated light-harvesting complexes, Biochemistry 40 (2001) 9902–9908.
[33] A.V. Ruban, J.P. Dekker, P. Horton, R. van Grondelle, Temperature dependence of chlorophyll fluorescence from the light harvesting complex II of higher plants, Photochem. Photobiol. 61 (1995) 216–221.
[34] A.V. Ruban, A.A. Pascal, B. Robert, Xanthophylls of the major photosynthetic light-harvesting complex of plants: identification, conformation and dynamics, FEBS Lett. 477 (2000) 181–185.
[35] S. Krawczyk, Z. Krupa, M. Maksymiec, Stark spectra of chlorophylls and carotenoids in antenna pigment-proteins LHC-II and CP-II, Biochim. Biophys. Acta 1143 (1993) 273–281.
[36] A.V. Ruban, A.J. Young, A.A. Pascal, P. Horton, The effects of illumination on the xanthophyll composition of the photosystem II light-harvesting complexes of spinach thylakoid membranes, Plant Physiol. 104 (1994) 227–234.
[37] G.U. Bublitz, S.G. Boxer, Stark spectroscopy: applications in chemistry, biology, and materials science, in: H.L. Strauss, G.T. Babcock, S.R. Leone (Eds.), Annu. Rev. Phys. Chem., vol. 48, 1997, pp. 213–242, Palo Alto, CA.
[38] M.L. Groot, R.N. Frese, F.L. de Weerd, K. Bromek, A. Pettersson, E.J.G. Peterman, I.H.M. van Stokkum, R. van Grondelle, J.P. Dekker, Spectroscopic properties of the CP43 core antenna protein of photosystem II, Biophys. J. 77 (1999) 3328–3340.
[39] R. Frese, U. Oberheide, I. van Stokkum, R. van Grondelle, M. Foidl, J. Oelze, H. van Amerongen, The organization of bacteriochlorophyll *c* in chlorosomes from *Chloroflexus aurantiacus* and the structural role of carotenoids and protein, Photosyn. Res. 54 (1997) 115–126.
[40] R. Mathies, L. Stryer, Retinal has a highly dipolar vertically excited singlet state: implications for vision, Proc. Natl. Acad. Sci. U. S. A. 73 (1976) 2169–2173.
[41] W. Liptay, Dipole moments and polarizabilities of molecules in excited states, in: E.C. Lim (Ed.), Excited States, vol. 1, Academic Press, New York, 1974, pp. 129–229.
[42] L.M.P. Beekman, M. Steffen, I.H.M. van Stokkum, J.D. Olsen, N. Hunter, S.G. Boxer, R. van Grondelle, Characterization of the light-harvesting antennas of photosynthetic purple bacteria by Stark spectroscopy: 1. LH1 antenna complex and the B820 subunit from *Rhodospirillum rubrum*, J. Phys. Chem., B 101 (1997) 7284–7292.
[43] C.C. Gradinaru, I.H.M. van Stokkum, R. van Grondelle, H. van Amerongen, Ultrafast absorption changes of the LHCII carotenoids upon selective excitation of the chlorophylls, in: G. Garab (Ed.),

Photosynthesis: Mechanisms and Effects, vol. 1, Kluwer Academic Publishing, Dordrecht, 1998, pp. 277–280.
[44] C.C. Gradinaru, R. van Grondelle, H. van Amerongen, Selective interaction between xanthophylls and chlorophylls in LHCII probed by femtosecond transient absorption spectrocopy, J. Phys. Chem. B 107 (2003) 3938–3943.
[45] M. Rätsep, T.W. Johnson, P.R. Chitnis, G.J. Small, The red-absorbing chlorophyll *a* antenna states of photosystem I: a hole-burning study of *Synechocystis* sp. PCC 6803 and its mutants, J. Phys. Chem. B 104 (2000) 836–847.
[46] R.B. Altmann, D. Haarer, I. Renge, Stark effect on spectral holes of chlorophyll *a* at 2 K, Chem. Phys. Lett. 216 (1993) 281–285.
[47] S. Krawczyk, Electrochromism of chlorophyll *a* monomer and special pair dimer, Biochim. Biophys. Acta 1056 (1991) 64–70.
[48] D. Lockhart, S.G. Boxer, Stark effect spectroscopy of *Rhodobacter sphaeroides* and *Rhodopseudomonas viridis* reaction centers, Proc. Natl. Acad. Sci. U. S. A. 85 (1988) 107–111.
[49] S. Krawczyk, D. Olszówka, Spectral broadening and its effect in Stark spectra of carotenoids, Chem. Phys. 265 (2001) 335–347.
[50] G. Garab, Z. Cseh, L. Kovács, S. Rajagopal, Z. Várkonyi, M. Wentworth, L. Mustárdy, A. Dér, A.V. Ruban, E. Papp, A. Holzenburg, P. Horton, Light-induced trimer to monomer transition in the main light-harvesting antenna complex of plants: thermo-optic mechanism, Biochemistry 41 (2002) 15121–15129.
[51] O.J.G. Somsen, R. van Grondelle, H. van Amerongen, Spectral broadening of interacting pigments: polarized absorption by photosynthetic proteins, Biophys. J. 71 (1996) 1934–1951.
[52] C.C. Gradinaru, I.H.M. van Stokkum, A.A. Pascal, R. van Grondelle, H. van Amerongen, Identifying the pathways of energy transfer between carotenoids and chlorophylls in LHCII and CP29. A multicolor, femtosecond pump-probe study, J. Phys. Chem. B 104 (2000) 9330–9342.